Electronic Supplementary Information (ESI)

Piroxicam-clonixin drug-drug cocrystal solvates with enhanced hydration stability

Duanxiu Li,[ab] Jiong Li,[b*] Zongwu Deng,[ab] and Hailu Zhang[ab*]

[a] *Laboratory of Magnetic Resonance Spectroscopy and Imaging, Suzhou Institute of Nano-Tech and Nano-Bionics, Chinese Academy of Sciences, Suzhou 215123, P. R. China. Tel: +86-512-62872713; Fax: +86-512-62603079; E-mail: hlzhang2008@sinano.ac.cn.*

[b] *CAS Key Laboratory of Nano-Bio Interface, Suzhou Institute of Nano-Tech and Nano-Bionics, Chinese Academy of Sciences, Suzhou 215123, P. R. China. E-mail: jli2006@sinano.ac.cn.*

Contents

Experimental section

Materials

Clonixin (CNX, form I, >98%) was purchased from TCI. Piroxicam (PXC, form α2, >98%) was purchased from Aladdin. All organic solvents of analytical grade were purchased from Sinopharm Chemical Reagent Co., Ltd. All chemicals were used without further purification.

Cocrystal screening

Method 1: Slurry experiment. Equimolar (0.5 mmol) of CNX and PXC were mixed in 2.5 mL of solvent and stirred for 3 days.

Method 2: Mechanochemical synthesis. Neat grinding and liquid-assisted grinding (LAG) experments (using the solvents in Table S1) were performed on a Pulverisette 23 (Fritsch, Germany) ball mill. Equimolar (0.5 mmol) of CNX and PXC were mixed in a 10-mL stainless steel jar with one 15-mm stainless steel grinding ball. For LAG experiments, the value of volume of solvent/sample weight was fixed at 0.30 μL/mg. Ball milling was performed at 40 Hz for 20 min.

Method 3: Solvent exchanging. 300 mg of PXC-CNX-MeCN was stirred in 2.5 mL of solvent (H_2O, MeOH, EtOH, i-PrOH, DMSO, EG, MPD, DOX, C_6H_6, C_7H_8, and PX) for 72 hours.

Synthesis of PXC-CNX-MeCN cocrystal solvate

Equimolar of CNX (131 mg, 0.5 mmol) and PXC (166 mg, 0.5 mmol) were mixed in 2.5 mL of MeCN and stirred for 3 days. The suspension was filtered and the isolated solids of PXC-CNX-MeCN were dried under a vacuum for 24 hours. The filtrate was left to evaporate slowly at room temperature. After several days, plate-shaped, light yellow crystals of PXC-CNX-MeCN were obtained.

Synthesis of PXC-CNX-AC cocrystal solvate

Equimolar of CNX (131 mg, 0.5 mmol) and PXC (166 mg, 0.5 mmol) were mixed in 2.5 mL of AC and stirred for 3 days. The suspension was filtered and the isolated solids of PXC-CNX-AC were dried under a vacuum for 24 hours. The filtrate was left to evaporate slowly at room temperature. After several days, plate-shaped, light yellow crystals of PXC-CNX-AC were obtained.

Synthesis of PXC-CNX-EA cocrystal solvate

Equimolar of CNX (131 mg, 0.5 mmol) and PXC (166 mg, 0.5 mmol) were mixed in 2.5 mL of EA and stirred for 3 days. The suspension was filtered and the isolated solids of PXC-CNX-EA were dried under a vacuum for 24 hours. The filtrate was left to evaporate slowly at room temperature. After several days, plate-shaped, light yellow crystals of PXC-CNX-EA were obtained.

Synthesis of PXC-CNX-$CHCl_3$ cocrystal solvate

Equimolar of CNX (131 mg, 0.5 mmol) and PXC (166 mg, 0.5 mmol) were mixed in 2.5 mL of $CHCl_3$ and stirred for 3 days. The suspension was filtered and the isolated solids of PXC-CNX-$CHCl_3$ were dried under a vacuum for 24 hours. The filtrate was left to evaporate slowly at room temperature. After several days, plate-shaped, light yellow crystals of PXC-CNX-$CHCl_3$ were obtained.

Synthesis of PXC-CNX-CH_2Cl_2 cocrystal solvate

Equimolar of CNX (131 mg, 0.5 mmol) and PXC (166 mg, 0.5 mmol) were mixed in 2.5 mL of CH_2Cl_2 and stirred for 3 days. The suspension was filtered and the isolated solids of PXC-CNX-CH_2Cl_2 were dried under a vacuum for 24 hours. The filtrate was left to evaporate slowly at room temperature. After several days, plate-shaped, light yellow crystals of PXC-CNX-CH_2Cl_2 were obtained.

Synthesis of PXC-CNX-DMF cocrystal solvate

Equimolar of CNX (262 mg, 1 mmol) and PXC (331 mg, 1 mmol) were mixed in 2.5 mL of DMF and stirred for 3 days. The suspension was filtered and the isolated solids of PXC-CNX-DMF were dried under a vacuum for 24 hours. The single crystal suitable for structure determination was not obtained.

Synthesis of PXC-CNX-THF cocrystal solvate

Equimolar of CNX (131 mg, 0.5 mmol) and PXC (166 mg, 0.5 mmol) were mixed in 2.5 mL of THF and stirred for 3 days. The suspension was filtered and the isolated solids of PXC-CNX-THF were dried under a vacuum for 24 hours. The single crystal suitable for structure determination was not obtained.

Powder X-ray diffraction (Powder XRD)

Powder XRD of all the samples were recorded on a Bruker D8 Advance X-ray powder diffractometer (Bruker AXS, Karlsruhe, Germany) equipped with a LynxEye detector (Cu Kα radiation). The tube current and voltage of the generator were set to

40 mA and 40 kV, respectively. The data were recorded over the 2θ range from 4° to 40° scanning with a step size of 0.0194° at ambient temperature.

Single crystal X-ray diffraction (Single crystal XRD)

Single crystal XRD measurements of PXC-CNX-MeCN, PXC-CNX-$CHCl_3$ and PXC-CNX-CH_2Cl_2 were made using an Xcalibur, Atlas, Gemini diffractometer (Agilent, Santa Clara, California) and the measurements of PXC-CNX-AC and PXC-CNX-EA were made using a Bruker APEX-II CCD diffractometer (Bruker AXS, Karlsruhe, Germany) with an enhanced X-ray source Mo Kα (λ = 0.71073 Å) at 193 K. The five crystal structures were solved by direct methods and refined on F^2 by full-matrix least-squares methods with the *SHELXL-2017* program.[1] All non-hydrogen atoms were refined anisotropically. Hydrogen atoms associated with carbon atoms were fixed in geometrically constrained positions. The active hydrogen atoms on the O/N−H groups of all structures were located from the difference Fourier maps. The summary of key crystallographic data and hydrogen bonding metrics are given in Table S2 and Table S3, respectively.

^{1}H liquid NMR

^{1}H liquid NMR spectra of all cocrystal solvates were acquired using a Varian 400 MHz spectrometer (Varian Inc. Palo Alto, CA) using DMSO-d6 as a solvent.

Thermogravimetric analysis (TGA) and differential scanning calorimetry (DSC)

TGA was performed on a Mettler Toledo TGA1 STAR System at a heating rate of 10 °C·min^{-1} under nitrogen. DSC was performed on a TA Discovery DSC 250 instrument. Samples were placed in sealed aluminum pans and heated at 10 °C·min^{-1} to 300 °C at a heating rate of 10 °C·min^{-1} under nitrogen atmosphere (50 mL·min^{-1}).

Moisture stability

PXC-CNX-EA and raw materials (CNX and PXC) were exposed under 95% RH conditions at 25 °C for 4 weeks. The resulting solids were subjected to powder XRD measurements to monitor possible phase transformation.

Energy framework calculation

The pairwise intermolecular interaction energy was estimated using *CrystalExplorer* and *Gaussian09W* with experimental crystal geometry.[2,3] Considering the uncertainty of hydrogen position by single crystal X-ray diffraction, the hydrogen positions were

normalized to standard neutron diffraction values during the calculation. The total intermolecular interaction energy for given molecule, is summed up the electrostatic, polarization, dispersion, and exchange-repulsion components terms with scale factors of 1.057, 0.740, 0.871, and 0.618.[4] The intermolecular interaction is neglected with molecule-molecule distance more than 3.8 Å.[5]

Table S1 The solvent property parameters and cocrystal screening results

	solvent	α	β	$E_T(30)$	New phase	Single crystal
1	water (H_2O) [a]	117	47	631	–	
2	methanol (MeOH) [b]	98	66	554	–	
3	ethanol (EtOH) [b]	86	75	519	–	
4	isopropanol (i-PrOH) [b]	76	84	492	–	
5	acetonitrile (MeCN) [b]	19	40	456	√	√
6	acetone (AC) [b]	08	43	422	√	√
7	ethyl acetate (EA) [b]	00	45	381	√	√
8	chloroform ($CHCl_3$) [b]	20	10	391	√	√
9	dichloromethane (CH_2Cl_2) [b]	13	10	407	√	√
10	N, N-dimethylformamide (DMF) [b]	00	69	438	√	⚑
11	tetrahydrofuran (THF) [b]	00	55	374	√	⚑
12	dimethyl sulfoxide (DMSO) [b]	00	76	451	–	
13	ethanediol (EG) [a]	90	52	563	–	
14	1,2-propanediol (MPD) [b]	83	78	541	–	
15	1,4-dioxane (DOX) [b]	00	37	360	–	
16	benzene (C_6H_6) [b]	00	10	343	–	⚑
17	toluene (C_7H_8, Tol) [b]	00	11	339	–	
18	para-xylene (PX) [b]	00	12	331	–	

[a] from ref. 6.

[b] from ref. 7.

"–" means a mixture of the starting materials in different forms: 1, PXC·H_2O+CNX I; 5, PXC α2+amorphous; 11, PXC·PX+CNX I; others, PXC α2+CNX I.

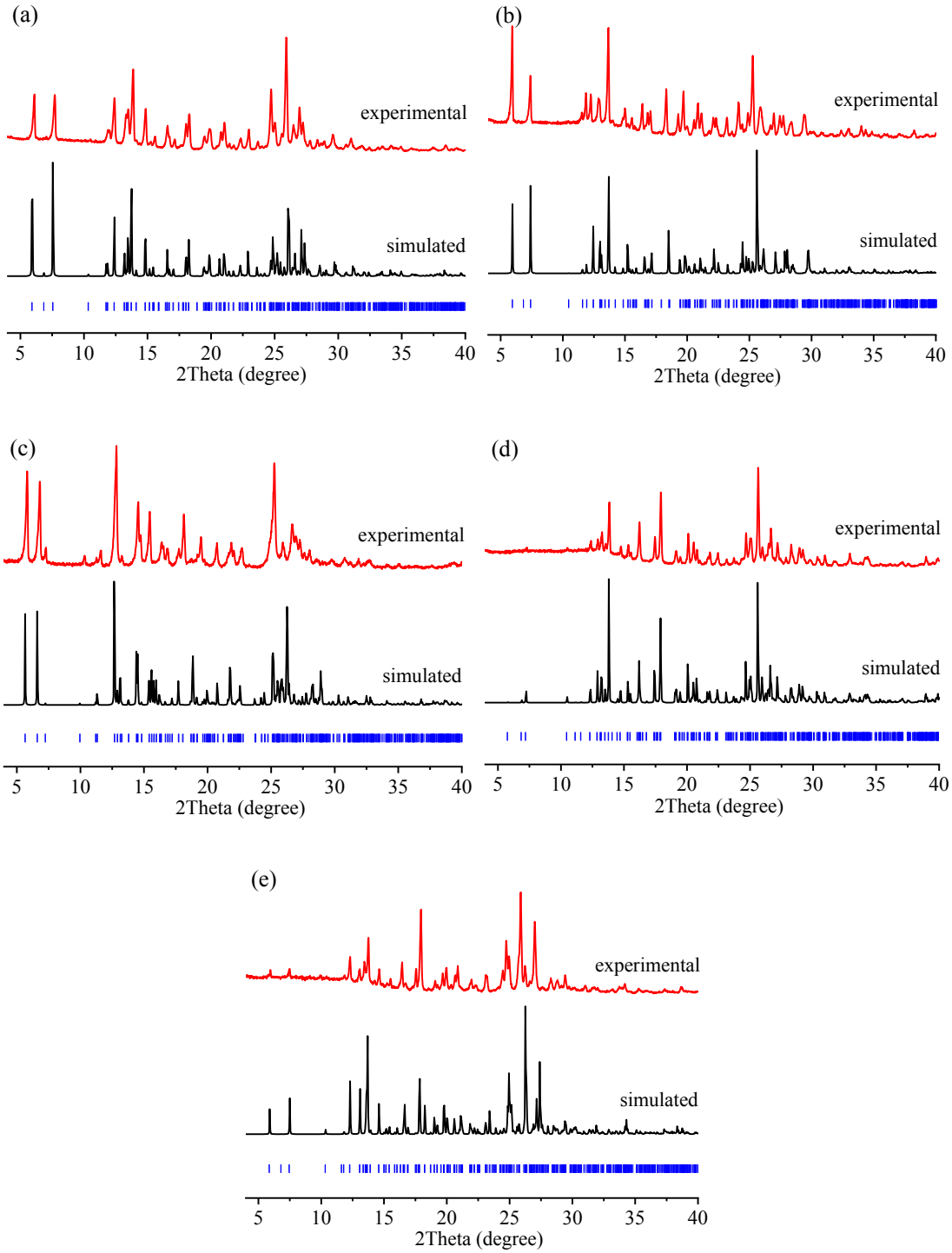

Fig. S1 Experimental and simulated powder XRD patterns of PXC-CNX-MeCN (a), PXC-CNX-AC (b), PXC-CNX-EA (c), PXC-CNX-$CHCl_3$ (d), and PXC-CNX-CH_2Cl_2 (e).

Table S2 Crystallographic data for five PXC-CNX cocrystal solvates

	PXC-CNX-MeCN	PXC-CNX-AC	PXC-CNX-EA	PXC-CNX-$CHCl_3$	PXC-CNX-CH_2Cl_2
Formula	$C_{30}H_{27}ClN_6O_6S$	$C_{31}H_{30}ClN_5O_7S$	$C_{32}H_{32}ClN_5O_8S$	$C_{29}H_{25}Cl_4N_5O_6S$	$C_{29}H_{26}Cl_3N_5O_6S$
Formula weight	635.08	652.11	682.13	713.40	678.96
Temperature/K	193(2)	193(2)	193(2)	193(2)	193(2)
Crystal system	Triclinic	Triclinic	Triclinic	Triclinic	Triclinic
Space group	*P*-1	*P*-1	*P*-1	*P*-1	*P*-1
a/Å	7.2364(8)	7.3032(5)	7.1077(7)	7.2799(5)	7.2499(2)
b/Å	13.684(2)	14.0521(8)	14.4856(13)	13.8946(11)	13.7111(6)
c/Å	15.767(2)	15.9432(11)	16.6126(15)	16.4922(13)	15.8281(7)
α/°	71.515(13)	69.237(2)	105.468(3)	68.131(7)	71.255(4)
β/°	83.596(10)	81.657(2)	98.006(3)	82.312(6)	85.172(3)
γ/°	81.899(11)	77.712(2)	103.645(3)	81.865(6)	83.669(3)
V/Å^3	1462.3(4)	1490.51(17)	1564.2(3)	1526.6(2)	1478.85(11)
Z	2	2	2	2	2
ρ_{calc}/(g·cm^{-3})	1.442	1.453	1.448	1.552	1.525
μ (Mo−Kα)/mm^{-1}	0.258	0.256	0.250	0.509	0.434
F (000)	660	680	712	732	700
total reflections	11946	23478	58082	19767	17757

unique reflections	5196 (R_{int} = 0.0540)	5375 (R_{int} = 0.0765)	7200 (R_{int} = 0.0657)	5977 (R_{int} = 0.0692)	5360 (R_{int} = 0.0343)
no. observations	3244	4015	5564	3367	4247
no. parameters	426	434	452	423	411
$R_1[I > 2\sigma(I)]/R_1$	0.0550/0.1017	0.0506/0.0781	0.0547/0.0789	0.0579/0.1175	0.0481/0.0625
$wR_2[I > 2\sigma(I)]/wR_2$	0.1097/0.1293	0.1368/0.1504	0.1240/0.1339	0.1186/0.1460	0.1344/0.1446
GOF	1.025	0.996	1.051	0.967	1.053
$\Delta\rho$max/$\Delta\rho$min (e Å^{-3})	0.259/-0.328	0.383/-0.405	0.385/-0.439	0.328/-0.303	0.643/-0.688
CCDC	1913246	1913247	1913248	1913249	1913250

Table S3 Hydrogen bond distances and angles for five PXC-CNX cocrystal solvates

	D—H···A	D—H/Å	H···A/Å	D···A/Å	D—H···A/º	Symmetry code
PXC-CNX-MeCN	N(2)—H(2A)···O(1)	0.88(3)	1.93(3)	2.685(4)	144(3)	
	O(2)—H(2C)···O(5)	0.91(4)	1.64(4)	2.532(3)	167(4)	
	N(4)—H(4A)···O(5)	0.90(3)	1.77(3)	2.549(3)	143(3)	
	N(5)—H(5A)···O(6)	0.93(4)	1.93(4)	2.638(4)	131(3)	
	N(5)—H(5A)···O(6)	0.93(4)	2.27(3)	2.918(3)	126(3)	-x+1, -y+2, -z+1
PXC-CNX-AC	N(2)—H(2A)···O(1)	0.92(3)	1.91(3)	2.701(3)	143(2)	
	O(2)—H(2C)···O(5)	1.02(3)	1.53(3)	2.552(2)	173(3)	
	N(4)—H(4A)···O(5)	0.84(3)	1.85(3)	2.575(3)	143(3)	
	N(5)—H(5A)···O(6)	0.82(3)	1.97(3)	2.623(3)	136(3)	
	N(5)—H(5A)···O(6)	0.82(3)	2.38(2)	2.932(2)	126(2)	-x+1, -y+2, -z+1
PXC-CNX-EA	N(2)—H(2A)···O(1)	0.83(3)	1.98(3)	2.702(2)	145(2)	
	O(2)—H(2C)···O(5)	0.94(4)	1.62(4)	2.545(2)	169(3)	
	N(4)—H(4A)···O(5)	0.90(3)	1.77(3)	2.551(2)	144(2)	
	N(5)—H(5A)···O(6)	0.90(3)	1.94(3)	2.641(2)	133(2)	
	N(5)—H(5A)···O(6)	0.90(3)	2.30(3)	2.913(2)	125(2)	-x+1, -y+2, -z+1
PXC-CNX-$CHCl_3$	N(2)—H(2A)···O(1)	0.82(3)	1.98(3)	2.698(4)	146(3)	
	O(2)—H(2C)···O(5)	0.99(5)	1.56(5)	2.545(3)	170(5)	

	N(4)—H(4A)···O(5)	0.92(4)	1.77(4)	2.555(4)	142(3)	
	N(5)—H(5A)···O(6)	0.89(4)	1.92(4)	2.634(4)	136(3)	
	N(5)—H(5A)···O(6)	0.89(4)	2.34(4)	2.929(4)	123(3)	-x+1, -y+2, -z+1
PXC-CNX-CH_2Cl_2	N(2)—H(2A)···O(1)	0.86(3)	1.94(3)	2.694(3)	146(3)	
	O(2)—H(2C)···O(5)	0.93(4)	1.62(4)	2.546(2)	171(4)	
	N(4)—H(4A)···O(5)	0.83(3)	1.83(3)	2.552(3)	145(3)	
	N(5)—H(5A)···O(6)	0.76(3)	2.07(3)	2.661(3)	135(3)	
	N(5)—H(5A)···O(6)	0.76(3)	2.39(3)	2.919(3)	128(3)	-x+1, -y, -z+1

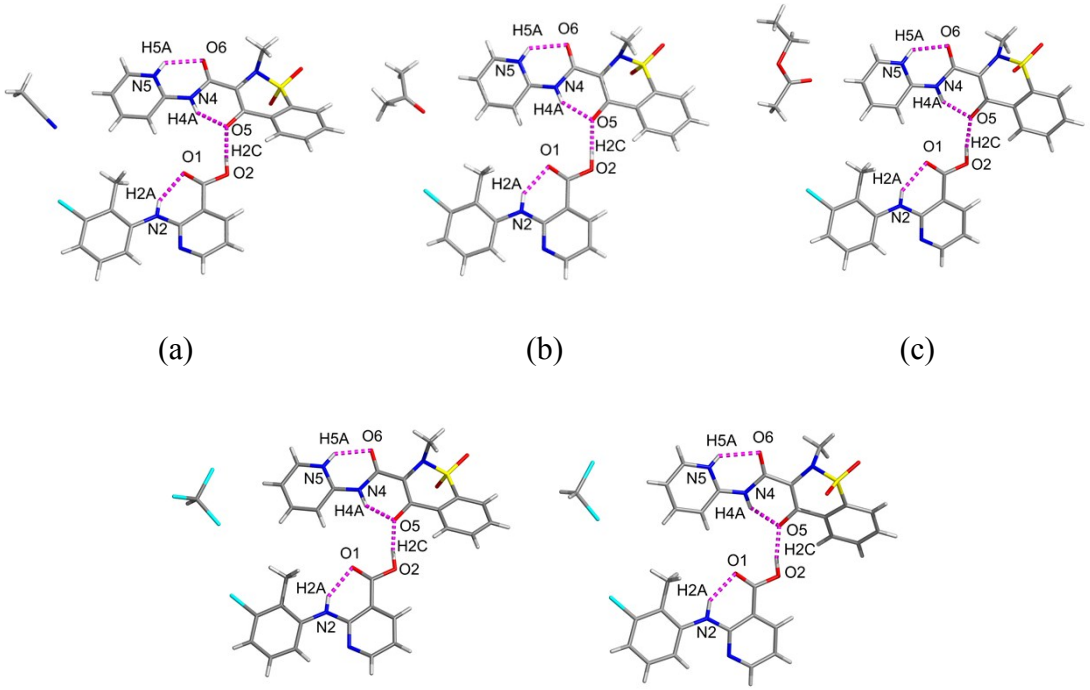

Fig. S2 The asymmetric units of PXC-CNX-MeCN (a), PXC-CNX-AC (b), PXC-CNX-EA (c), PXC-CNX-$CHCl_3$ (d), and PXC-CNX-CH_2Cl_2 (e).

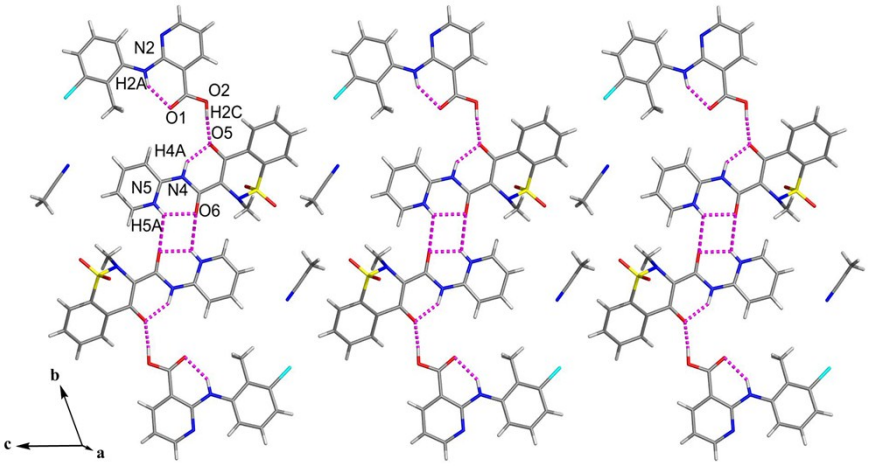
N2
H2A
O1
O2
H2C
O5
H4A
N5
N4
O6
H5A
b
c
a

(a)

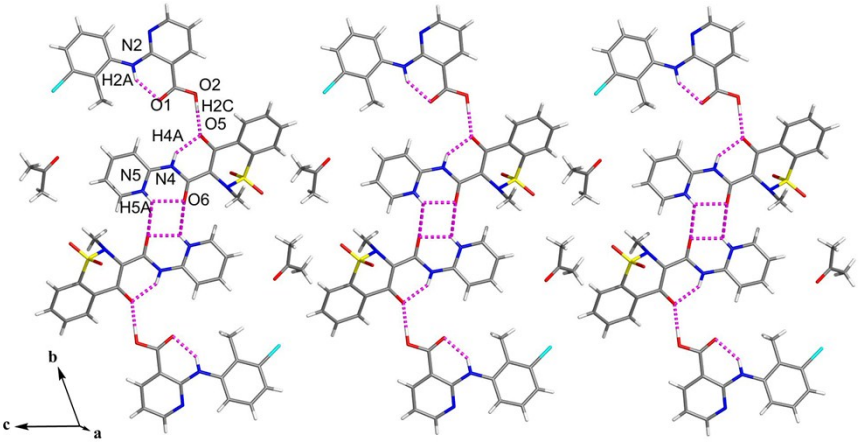
N2
H2A
O1
O2
H2C
O5
H4A
N5
N4
O6
H5A
b
c
a

(b)

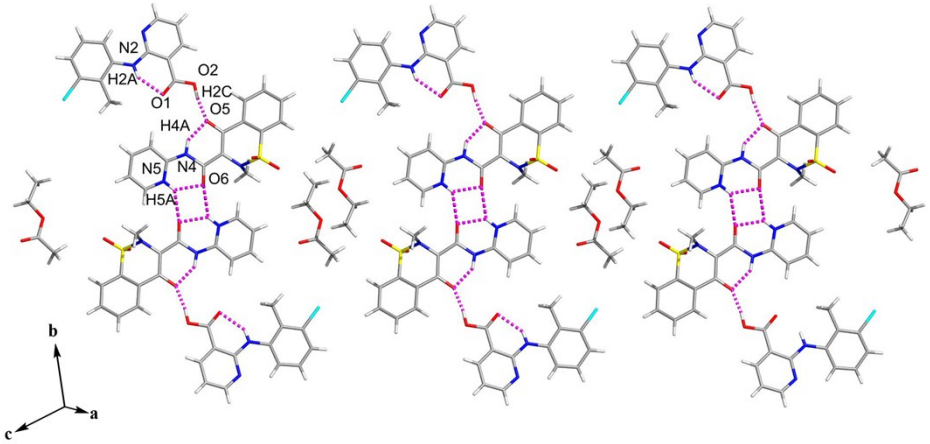
N2
H2A
O1
O2
H2C
O5
H4A
N5
N4
O6
H5A
b
c
a

(c)

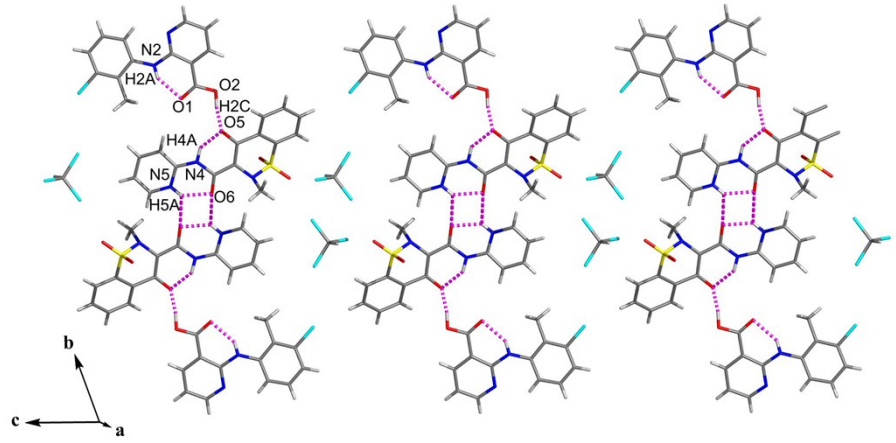

(d)

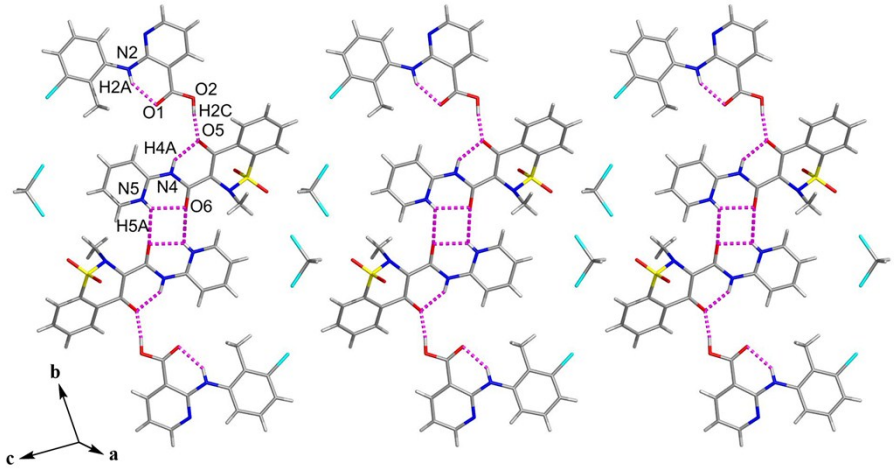

(e)

Fig. S3 1D molecular tape structures of PXC-CNX-MeCN (a), PXC-CNX-AC (b), PXC-CNX-EA (c), PXC-CNX-$CHCl_3$ (d), and PXC-CNX-CH_2Cl_2 (e).

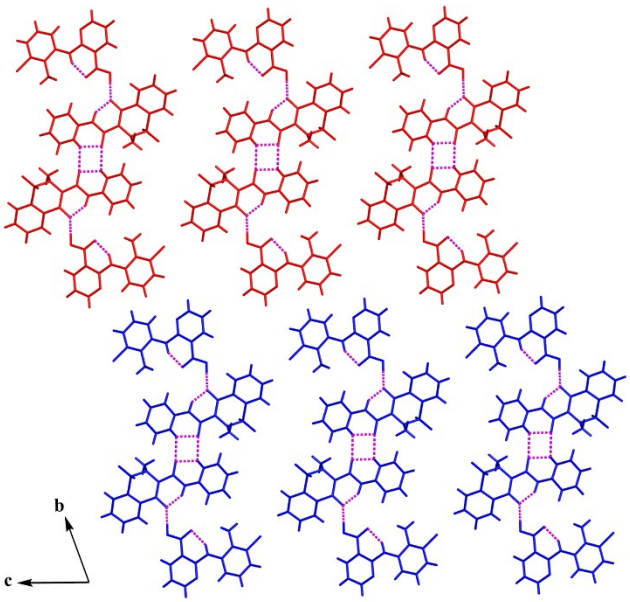

(a)

(b)

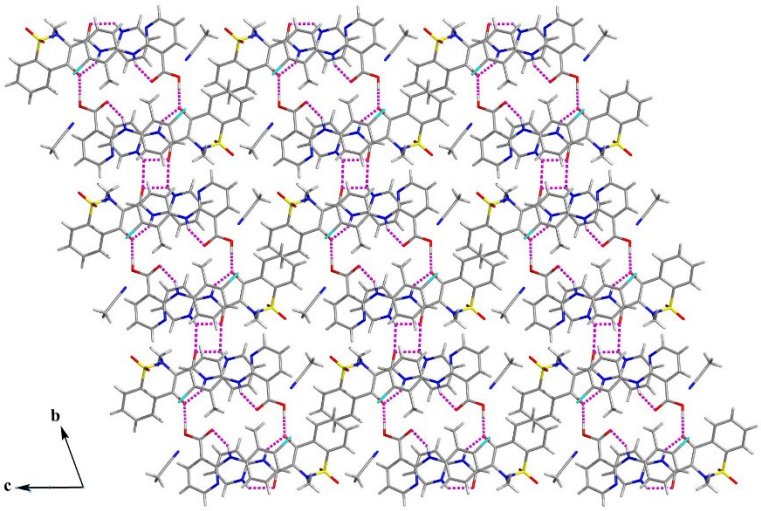

(c)

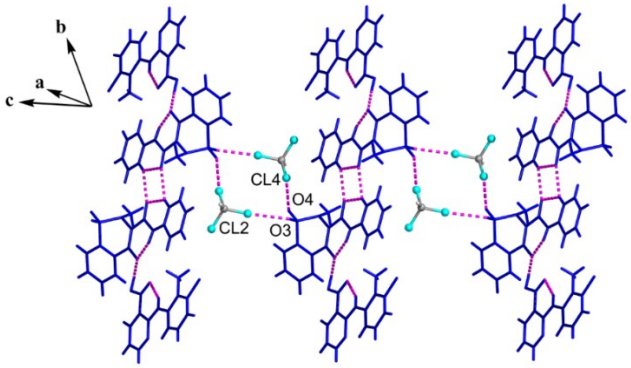

(d)

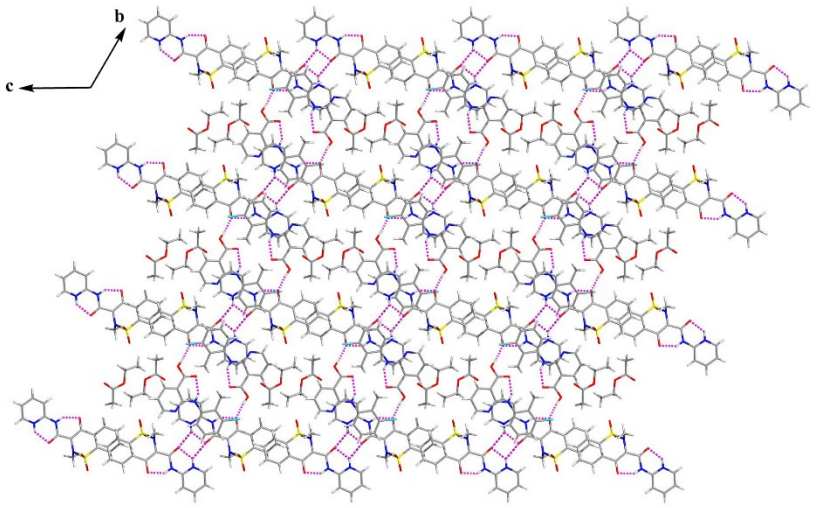

(e)

Fig. S4 Two adjacent PXC-CNX molecular tapes in the same plane (a), the parallel packing of four PXC-CNX molecular tapes (b), and 3D packing structure of PXC-CNX-MeCN viewed along the *a* axis (c). Halogen-bond interactions in PXC-CNX-$CHCl_3$ (d). 3D packing structure of PXC-CNX-EA viewed along the *a* axis (e).

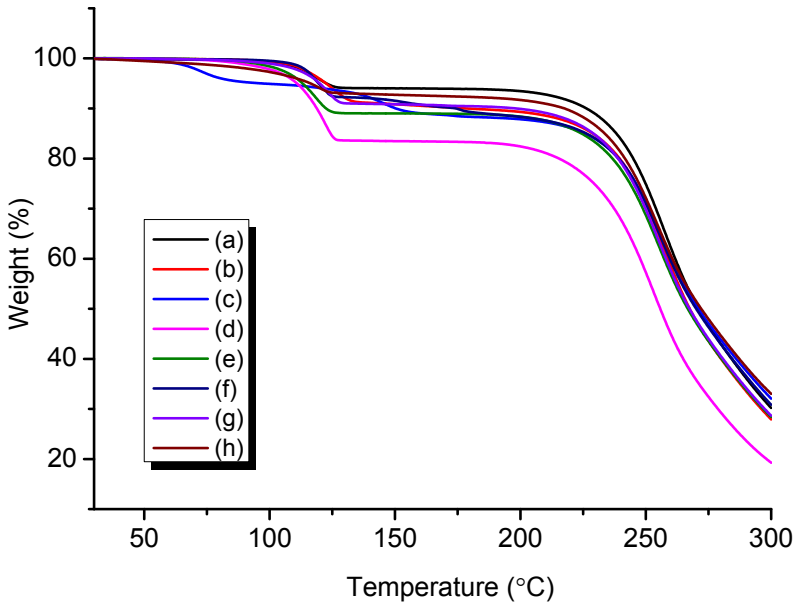

Fig. S5 TG analysis curves for PXC-CNX-MeCN (a), PXC-CNX-AC (b), PXC-CNX-EA (c), PXC-CNX-$CHCl_3$ (d), PXC-CNX-CH_2Cl_2 (e), PXC-CNX-DMF (f), PXC-CNX-THF (g), and PXC-CNX-0.5C_6H_6 (h).

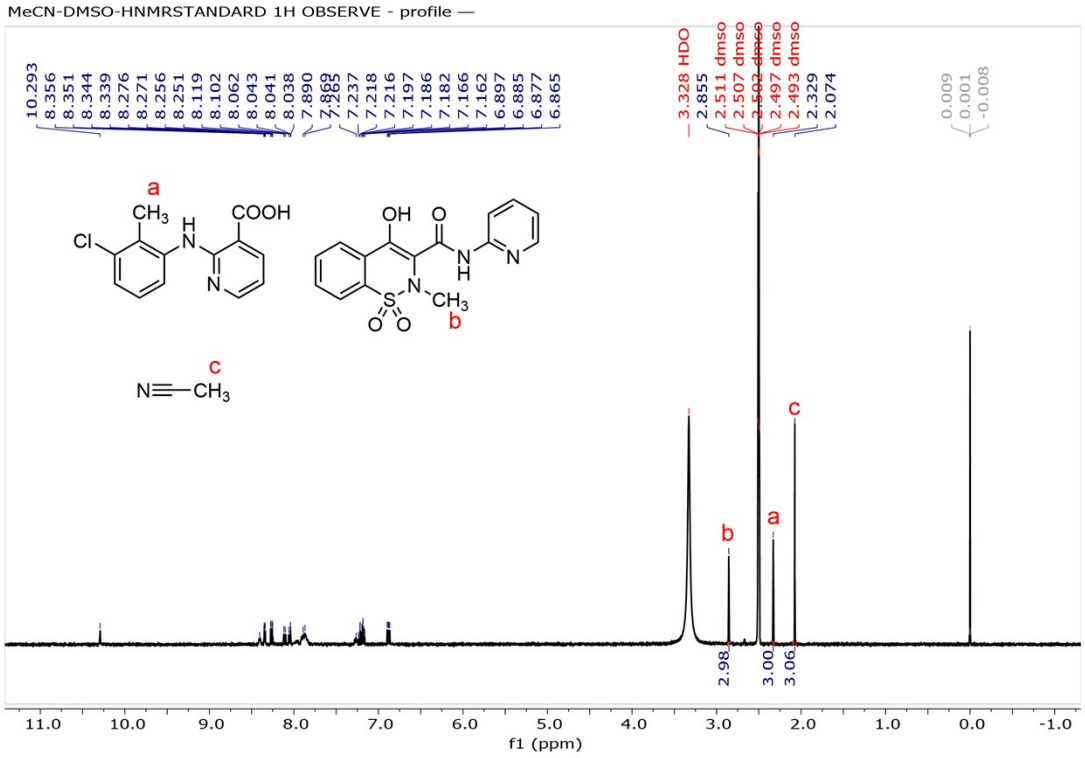
MeCN-DMSO-HNMRSTANDARD 1H OBSERVE - profile —
10.293
8.356
8.351
8.344
8.339
8.276
8.271
8.256
8.251
8.119
8.102
8.062
8.043
8.041
8.038
7.890
7.869
7.865
7.237
7.218
7.216
7.197
7.186
7.182
7.166
7.162
6.897
6.885
6.877
6.865
3.328 HDO
2.855
2.511 dmso
2.507 dmso
2.501 dmso
2.497 dmso
2.493 dmso
2.329
2.074
0.009
0.001
-0.008
a
b
c
2.98
3.00
3.06
11.0
10.0
9.0
8.0
7.0
6.0
5.0
4.0
3.0
2.0
1.0
0.0
-1.0
f1 (ppm)

(a)

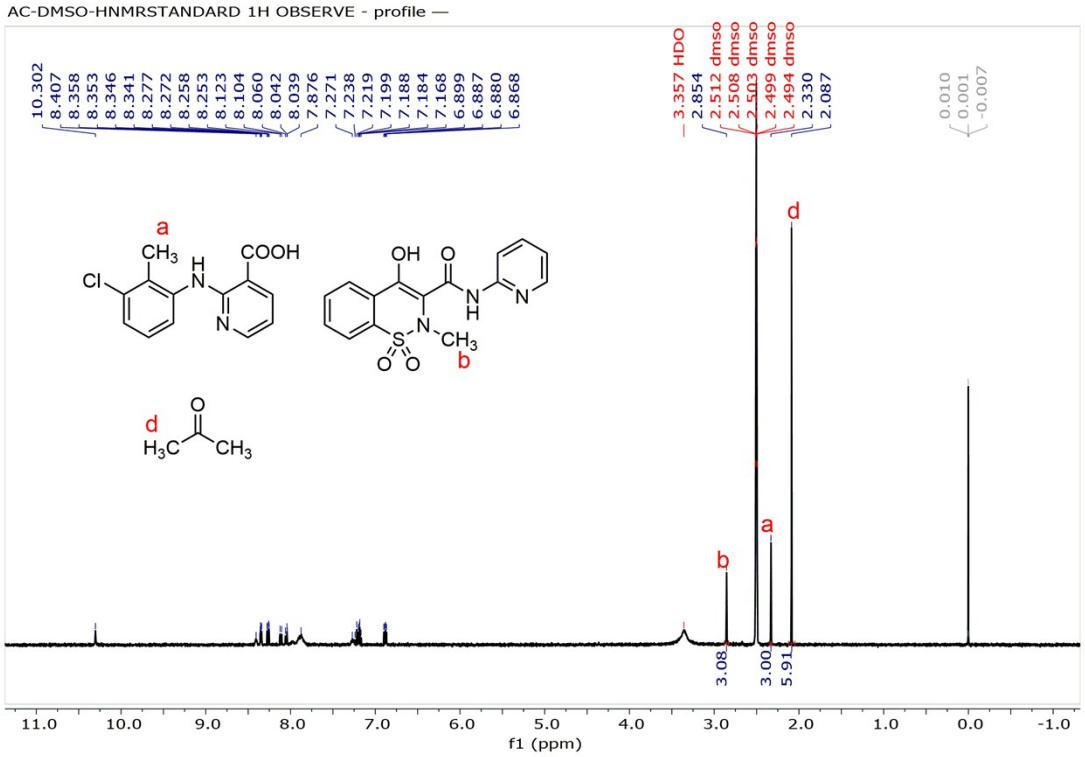
AC-DMSO-HNMRSTANDARD 1H OBSERVE - profile —
10.302
8.407
8.358
8.353
8.346
8.341
8.277
8.272
8.258
8.253
8.123
8.104
8.060
8.042
8.039
7.876
7.271
7.238
7.219
7.199
7.188
7.184
7.168
6.899
6.887
6.880
6.868
3.357 HDO
2.854
2.512 dmso
2.508 dmso
2.503 dmso
2.499 dmso
2.494 dmso
2.330
2.087
0.010
0.001
-0.007
a
b
d
3.08
3.00
5.91
11.0
10.0
9.0
8.0
7.0
6.0
5.0
4.0
3.0
2.0
1.0
0.0
-1.0
f1 (ppm)

(b)

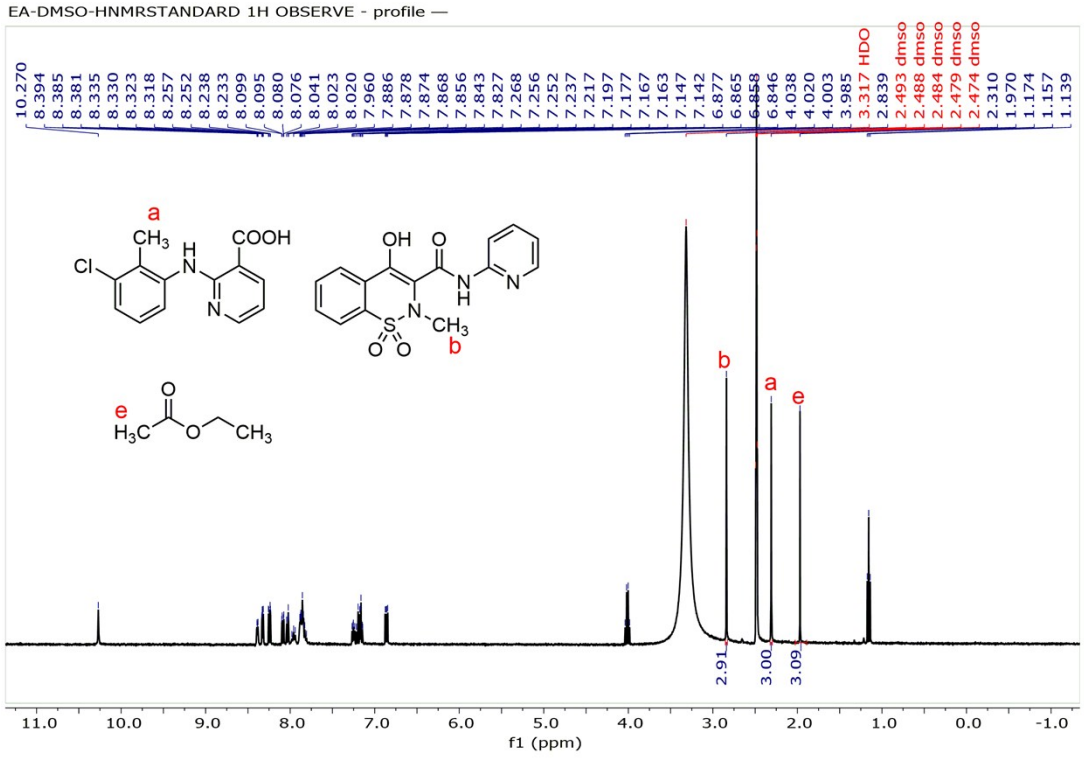
EA-DMSO-HNMRSTANDARD 1H OBSERVE - profile —
10.270
8.394
8.385
8.381
8.335
8.330
8.323
8.318
8.257
8.252
8.238
8.233
8.099
8.095
8.080
8.076
8.041
8.023
8.020
7.960
7.886
7.878
7.874
7.868
7.856
7.843
7.827
7.268
7.256
7.252
7.237
7.217
7.197
7.177
7.167
7.163
7.147
7.142
6.877
6.865
6.858
6.846
4.038
4.020
4.003
3.985
3.317 HDO
2.839
2.493 dmso
2.488 dmso
2.484 dmso
2.479 dmso
2.474 dmso
2.310
1.970
1.174
1.157
1.139
a
CH3
H
N
COOH
Cl
N
OH
O
N
H
N
S
N
CH3
O
O
b
e
H3C
O
O
CH3
b
a
e
2.91
3.00
3.09
11.0
10.0
9.0
8.0
7.0
6.0
5.0
4.0
3.0
2.0
1.0
0.0
-1.0
f1 (ppm)

(c)

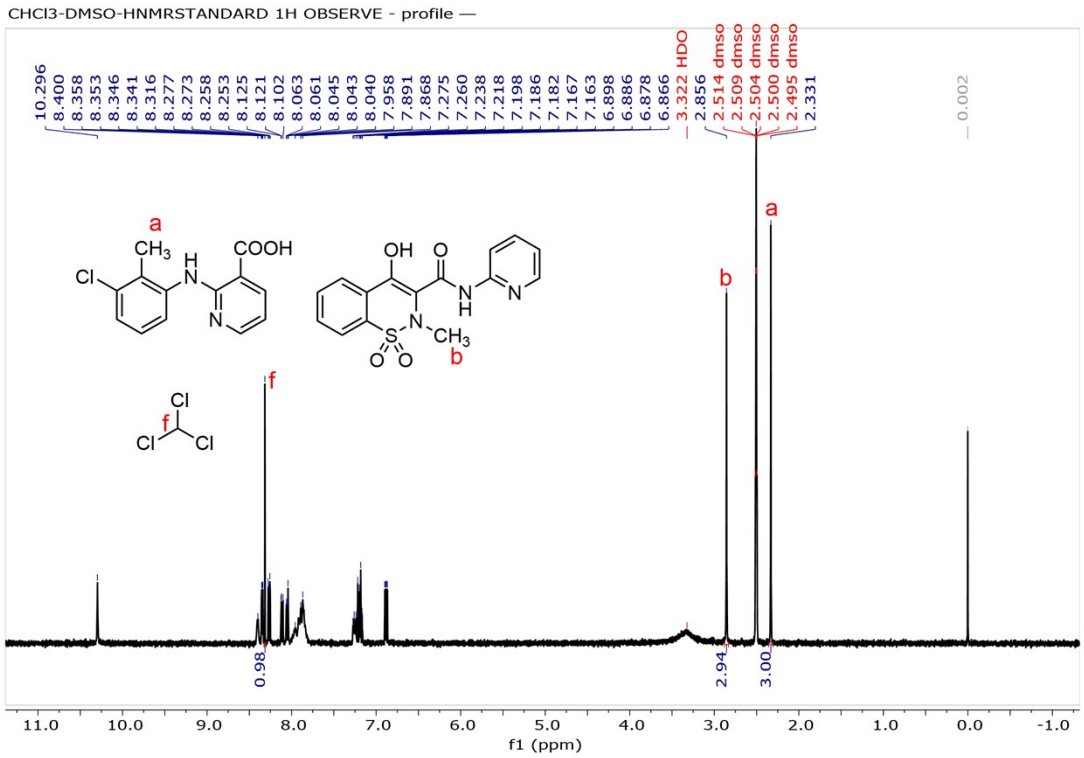
CHCl3-DMSO-HNMRSTANDARD 1H OBSERVE - profile —
10.296
8.400
8.358
8.353
8.346
8.341
8.316
8.277
8.273
8.258
8.253
8.125
8.121
8.102
8.063
8.061
8.045
8.043
8.040
7.958
7.891
7.868
7.275
7.260
7.238
7.218
7.198
7.186
7.182
7.167
7.163
6.898
6.886
6.878
6.866
3.322 HDO
2.856
2.514 dmso
2.509 dmso
2.504 dmso
2.500 dmso
2.495 dmso
2.331
0.002
a
CH3
H
N
COOH
Cl
N
OH
O
N
H
N
S
N
CH3
O
O
b
f
Cl
f
Cl
Cl
b
a
0.98
2.94
3.00
11.0
10.0
9.0
8.0
7.0
6.0
5.0
4.0
3.0
2.0
1.0
0.0
-1.0
f1 (ppm)

(d)

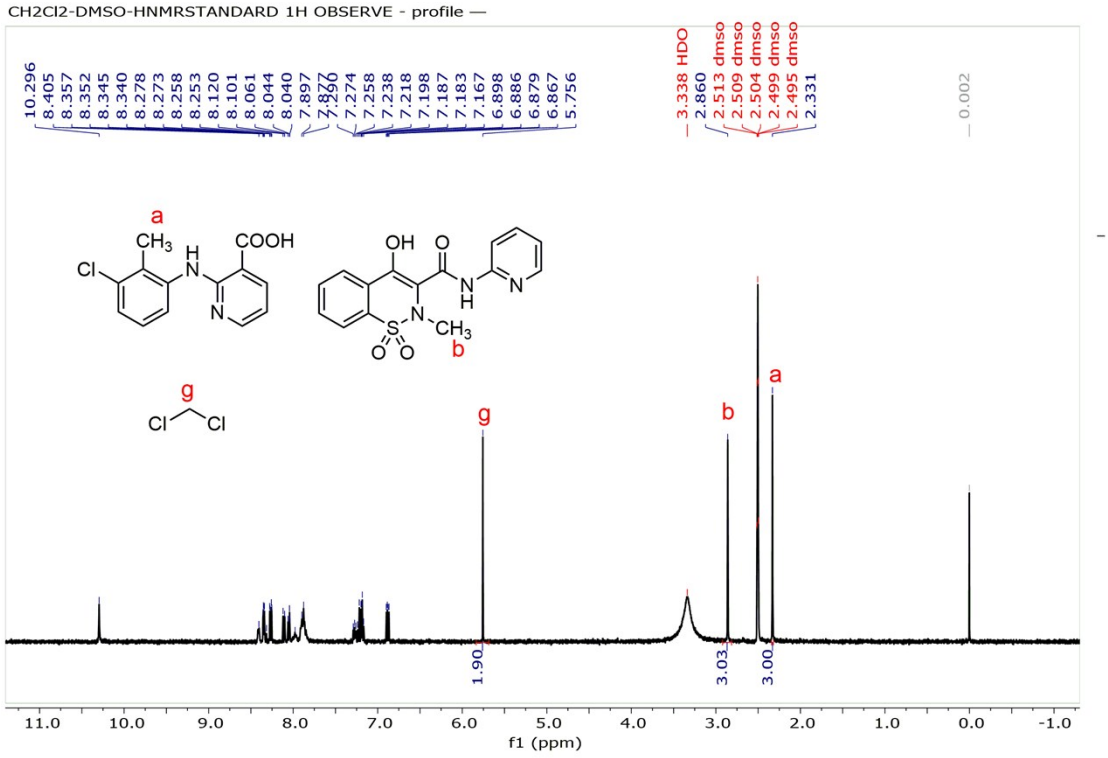
CH2Cl2-DMSO-HNMRSTANDARD 1H OBSERVE - profile
10.296
8.405
8.357
8.352
8.345
8.340
8.278
8.273
8.258
8.253
8.120
8.101
8.061
8.044
8.040
7.897
7.877
7.274
7.258
7.238
7.218
7.198
7.187
7.183
7.167
6.898
6.886
6.879
6.867
5.756
3.338 HDO
2.860
2.513 dmso
2.509 dmso
2.504 dmso
2.499 dmso
2.495 dmso
2.331
0.002
a
CH3
H
N
COOH
Cl
N
OH
O
N
H
N
S
N
CH3
O
O
b
g
Cl
Cl
g
b
a
1.90
3.03
3.00
11.0
10.0
9.0
8.0
7.0
6.0
5.0
4.0
3.0
2.0
1.0
0.0
-1.0
f1 (ppm)

(e)

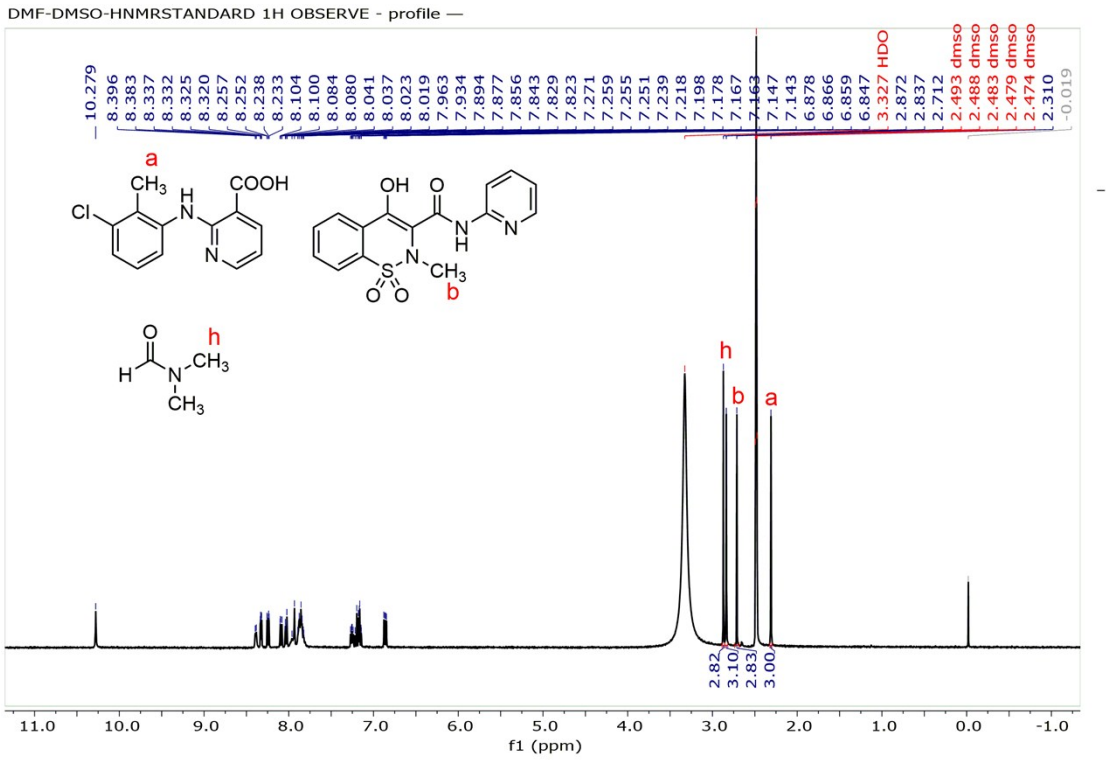
DMF-DMSO-HNMRSTANDARD 1H OBSERVE - profile
10.279
8.396
8.383
8.337
8.332
8.325
8.320
8.257
8.252
8.238
8.233
8.104
8.100
8.084
8.080
8.041
8.037
8.023
8.019
7.963
7.934
7.894
7.877
7.856
7.843
7.829
7.823
7.271
7.259
7.255
7.251
7.239
7.218
7.198
7.178
7.167
7.163
7.147
7.143
6.878
6.866
6.859
6.847
3.327 HDO
2.872
2.837
2.712
2.493 dmso
2.488 dmso
2.483 dmso
2.479 dmso
2.474 dmso
2.310
-0.019
a
CH3
H
N
COOH
Cl
N
OH
O
N
H
N
S
N
CH3
O
O
b
O
h
H
N
CH3
CH3
h
b
a
2.82
3.10
2.83
3.00
11.0
10.0
9.0
8.0
7.0
6.0
5.0
4.0
3.0
2.0
1.0
0.0
-1.0
f1 (ppm)

(f)

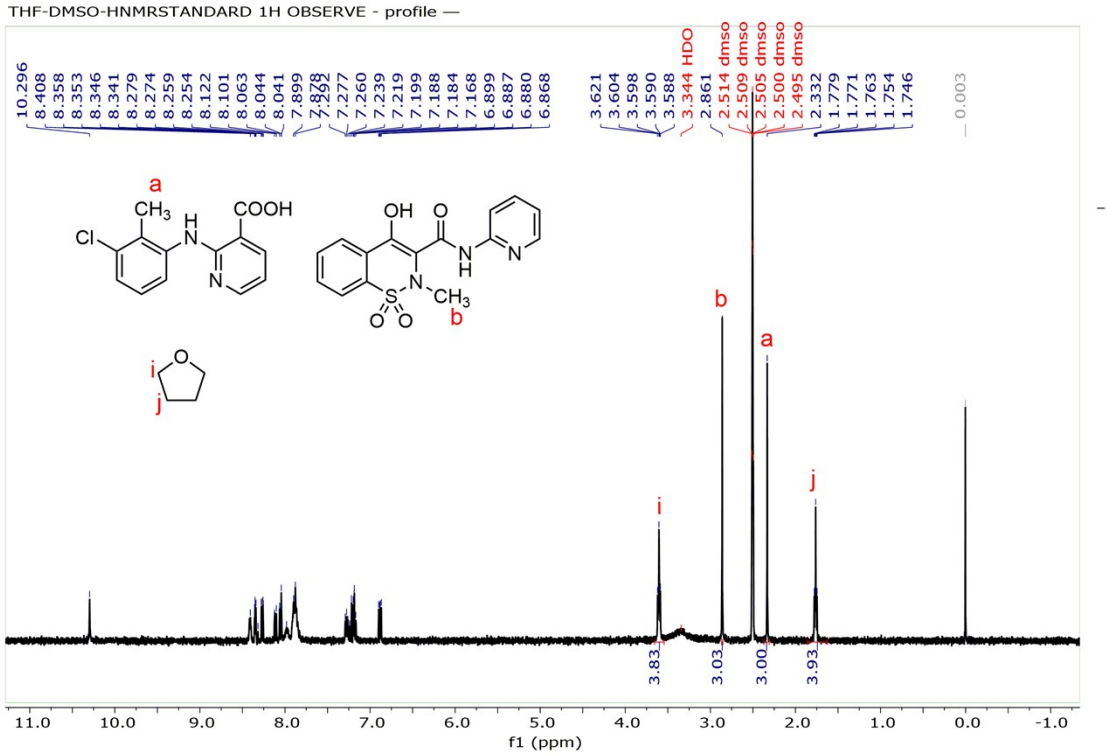

(g)

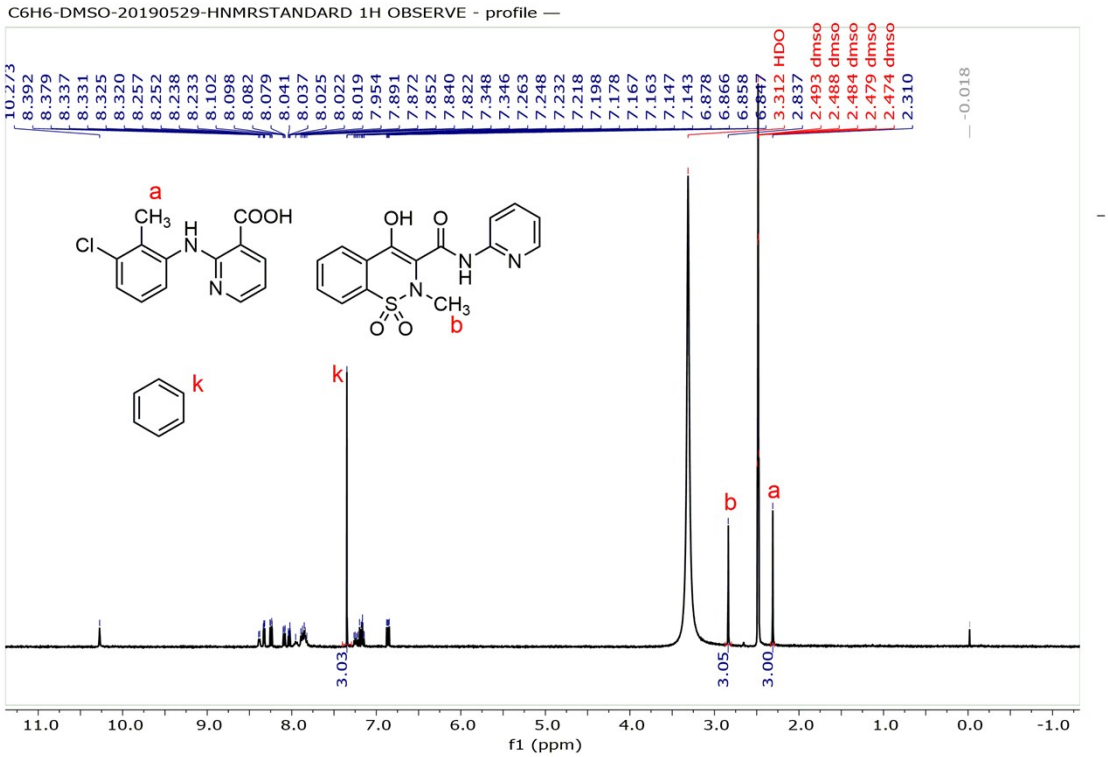

(h)

Fig. S6 Liquid ^{1}H NMR spectra of the 8 cocrystal solvates. PXC-CNX-MeCN (a), PXC-CNX-AC (b), PXC-CNX-EA (c), PXC-CNX-$CHCl_3$ (d), PXC-CNX-CH_2Cl_2 (e), PXC-CNX-DMF (f), PXC-CNX-THF (g), and PXC-CNX-0.5C_6H_6 (h).

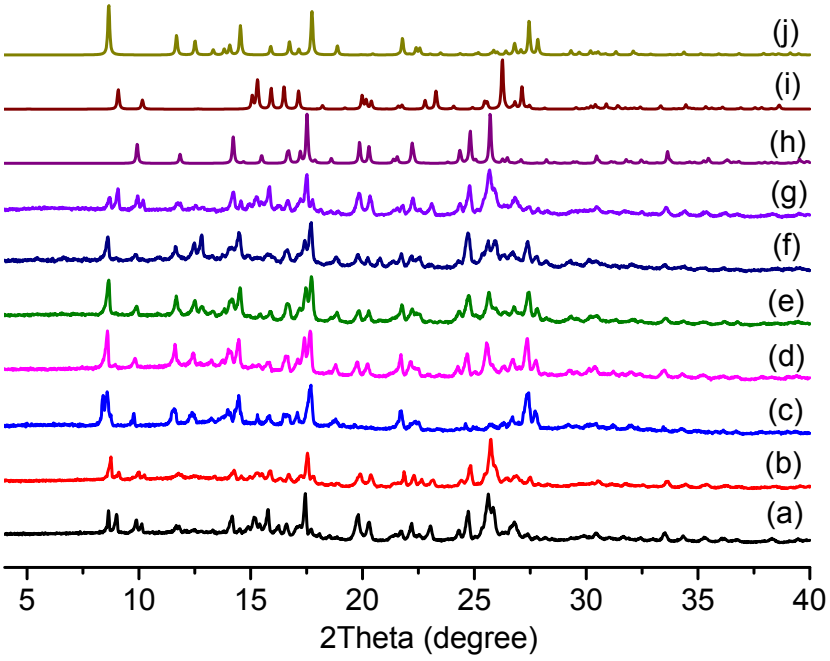

Fig. S7 Powder XRD patterns of desolvated PXC-CNX-MeCN (a), PXC-CNX-AC (b), PXC-CNX-EA (c), PXC-CNX-$CHCl_3$ (d), PXC-CNX-CH_2Cl_2 (e), PXC-CNX-THF (f), and PXC-CNX-$0.5C_6H_6$ (g). The simulated patterns for CNX form I (h), PXC form α2 (i), and PXC form I (j) are also provided. In some samples, trace amounts of residual solvates (feature diffraction peak at ~13°) are also present.

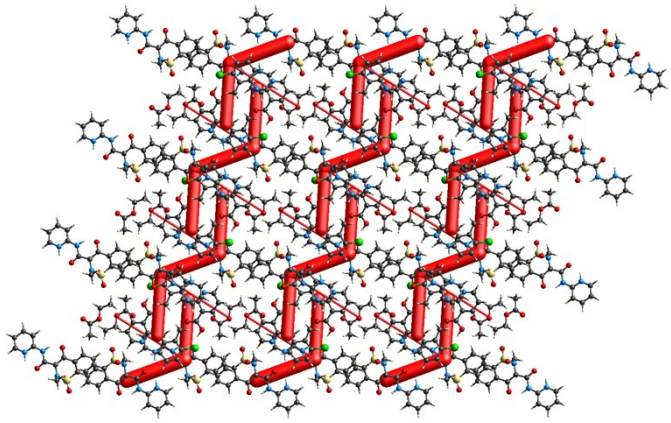

(a)

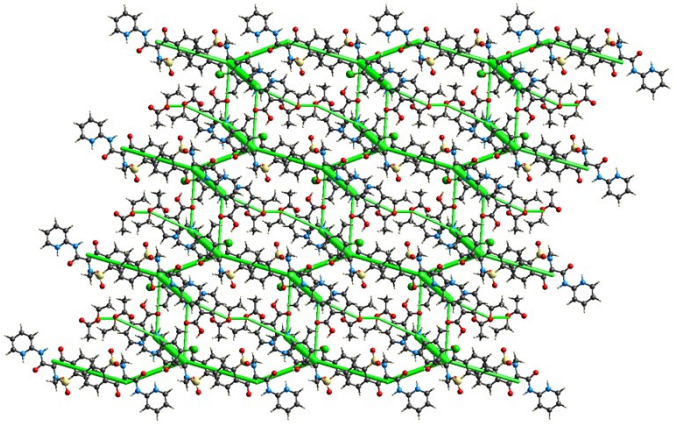

(b)

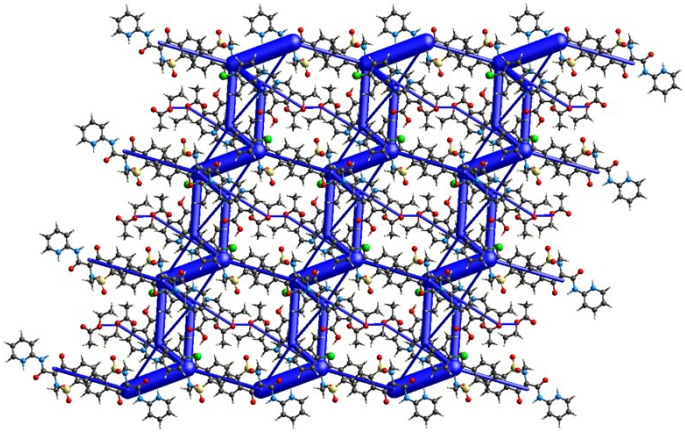

(c)

Fig. S8 Energy framework diagrams for separate electrostatic (a) and dispersion (b) contributions to the total interaction energies (c) in PXC-CNX-EA. The thickness of each cylinder represents the relative strength of interaction. The energy threshold for the energy framework is set at −15 kJ mol^{-1}.

Table S4 Intermolecular interaction energies (kJ mol^{-1}) of PXC-CNX-EA cocrystal solvate estimated using B3LYP/6-31G (d, p) dispersion-corrected DFT models (CNX as a central molecule).

□	Number	Molecule	N	Symop	R	E_ele	E_pol	E_dis	E_rep	E_tot
□	1	PXC	1	-	6.19	-11.8	-13.3	-64.4	43.6	-51.5
□	2	PXC	1	-	7.68	-0.5	-1.9	-15.2	5.8	-11.6
□	3	CNX	1	-x, -y, -z	8.72	-2.7	-0.3	-12.8	5.9	-10.5
□	4	PXC	1	-	5.5	-2.6	-5.9	-71.7	42.4	-43.4
□	5	CNX	1	-x, -y, -z	6.84	-6.8	-0.8	-11.5	1.6	-16.8
□	6	EA	1	-	8.78	-1.1	-0.5	-4.7	2.3	-4.2
□	7	PXC	1	-	13.17	-0.6	-0.4	-5	3.3	-3.1
□	8	PXC	1	-	7.88	-14.1	-5.5	-11.1	11.5	-21.6
□	9	CNX	1	-x, -y, -z	6.62	-8.7	-1.1	-16.6	6.1	-20.6
□	10	PXC	1	-	8.08	-95.5	-23.8	-24.1	107.3	-73.3
□	11	EA	1	-	5.91	-4	-1.1	-25.4	19.8	-14.9
□	12	PXC	1	-	13.66	0	-0.1	-1.2	0	-1.1
□	13	EA	1	-	7.79	0.7	-1.1	-7.2	2.5	-4.8
□	14	EA	1	-	8.96	-1.8	-0.5	-9.6	7	-6.3

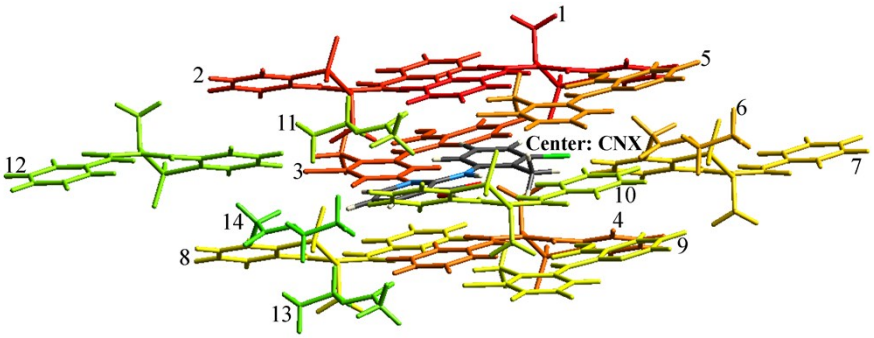

Table S5 Intermolecular interaction energies (kJ mol^{-1}) of PXC-CNX-EA cocrystal solvate estimated using B3LYP/6-31G (d, p) dispersion-corrected DFT models (PXC as a central molecule).

□	Number	Molecule	N	Symop	R	E_ele	E_pol	E_dis	E_rep	E_tot
□	1	CNX	1	-	6.19	-11.8	-13.3	-64.4	43.6	-51.5
□	2	EA	1	-	10.39	-16.5	-4.9	-9.6	12	-22.1
□	3	PXC	1	-x, -y, -z	7.95	-109.6	-29.4	-44.1	63.1	-137.1
□	4	PXC	2	x, y, z	7.11	11.5	-3.7	-6.7	1.6	4.6
□	5	CNX	1	-	8.08	-95.5	-23.8	-24.1	107.3	-73.3
□	6	CNX	1	-	5.5	-2.6	-5.9	-71.7	42.4	-43.4
□	7	PXC	1	-x, -y, -z	9.53	-13.9	-6.3	-31.2	24.7	-31.2
□	8	EA	1	-	7.8	-3.8	-0.7	-7.2	3.2	-8.8
□	9	EA	1	-	10.29	-0.5	-0.1	-5.1	3.9	-2.7
□	10	CNX	1	-	13.66	0	-0.1	-1.2	0	-1.1
□	11	PXC	1	-x, -y, -z	9.87	-4.3	-1.4	-37.2	23.7	-23.3
□	12	CNX	1	-	7.88	-14.1	-5.5	-11.1	11.5	-21.6
□	13	CNX	1	-	7.68	-0.5	-1.9	-15.2	5.8	-11.6
□	14	EA	1	-	7.97	-4.6	-3.2	-10	6.8	-11.7
□	15	CNX	1	-	13.17	-0.6	-0.4	-5	3.3	-3.1
□	16	EA	1	-	8.53	-3.2	-2.1	-8.8	7.5	-7.9
□	17	EA	1	-	9.03	-0.1	-0.1	-1.7	0	-1.6

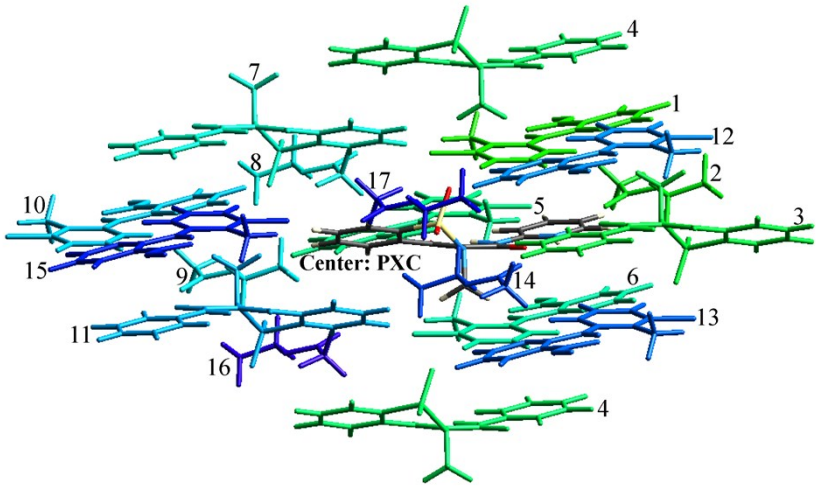

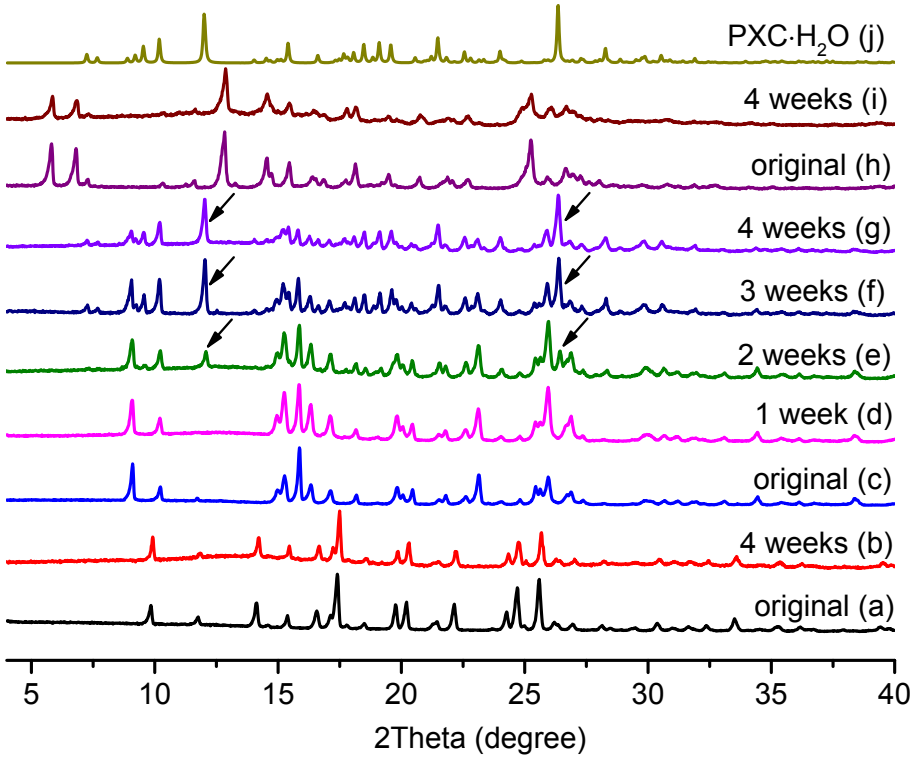

Fig. S9 Powder XRD patterns of CNX (a and b), PXC (c–g), and PXC-CNX-EA (h and i) before and after equilibration at 95% RH/25 °C for different periods. Simulated powder XRD pattern of PXC·H_2O (j) is also provided.

References

1 G. M. Sheldrick, Crystal structure refinement with SHELXL. *Acta Cryst. C*, **2015**, *71*, 3−8.

2 M. J. Turner, J. J. McKinnon, S. K. Wolff, D. J. Grimwood, P. R. Spackman, D. Jayatilaka and M. A. Spackman. **2017**. CrystalExplorer17. University of Western Australia.

3 M. J. Frisch, G. W. Trucks, H. B. Schlegel, G. E. Scuseria, M. A. Robb, J. R. Cheeseman, G. Scalmani, V. Barone, B. Mennucci, G. A. Petersson, H. Nakatsuji, M. Caricato, X. Li, H. P. Hratchian, A. F. Izmaylov, J. Bloino, G. Zheng, J. L. Sonnenberg, M. Hada, M. Ehara, K. Toyota, R. Fukuda, J. Hasegawa, M. Ishida, T. Nakajima, Y. Honda, O. Kitao, H. Nakai, T. Vreven, Jr. J. A. Montgomery, J. E. Peralta, F. Ogliaro, M. Bearpark, J. J. Heyd, E. Brothers, K. N. Kudin, V. N. Staroverov, R. Kobayashi, J. Normand, K. Raghavachari, A. Rendell, J. C. Burant, S. S. Iyengar, J. Tomasi, M. Cossi, N. Rega, J. M. Millam, M. Klene, J. E.Knox, J. B. Cross, V. Bakken, C. Adamo, J. Jaramillo, R. E. Gomperts, O. Stratmann, A. J. Yazyev, R. Austin, C. Cammi, J. W. Pomelli, R. Ochterski, R. L. Martin, K. Morokuma, V. G. Zakrzewski, G. A. Voth, P. Salvador, J. J. Dannenberg, S. Dapprich, A. D. Daniels, O. Farkas, J. B. Foresman, J. V. Ortiz, J. Cioslowski, D. J. Fox, Gaussian 09, Revision A. (**2009**), Gaussian, Inc., Wallingford CT.

4 M. J. Turner, S. Grabowsky, D. Jayatilaka, M. A. Spackman, Accurate and efficient model energies for exploring intermolecular interactions in molecular crystals. *J. Phys. Chem. Lett.,* **2014**, *5*(24), 4249−4255.

5 M. J. Turner, S. P. Thomas, M. W. Shi, D. Jayatilaka, M. A. Spackman, Energy frameworks: insights into interaction anisotropy and the mechanical properties of molecular crystals. *Chem. Comm.,* **2015**, *51*(18), 3735−3738.

6 Y. Marcus, *Ed. Wiley*: The Properties of Solvents, **1998**.

7 Y. Marcus, The properties of organic liquids that are relevant to their use as solvating solvents. *Chem. Soc. Rev.,* **1993**, *22* (6), 409−416.